https://doi.org/10.5194/acp-2019-1218
Preprint. Discussion started: 13 February 2020

Atmospheric Chemistry and Physics Discussions

Temperature Effects on Optical Properties and Chemical Composition of Secondary Organic Aerosol Derived from *n*-Dodecane

Junling Li[1,2,4], Weigang Wang[*,1,2], Kun Li[5], Wenyu Zhang[1,2], Chao Peng[1,2], Li Zhou[6], Bo Shi[1,2], Yan Chen[1,2], Mingyuan Liu[1,2], Hong Li[4], Maofa Ge[1,2,3]

[1]State Key Laboratory for Structural Chemistry of Unstable and Stable Species, Beijing National Laboratory for Molecular Sciences (BNLMS), CAS Research/Education Center for Excellence in Molecular Sciences, Institute of Chemistry, Chinese Academy of Sciences, Beijing 100190, P. R. China
[2] University of Chinese Academy of Sciences, Beijing 100049, P. R. China
[3] Center for Excellence in Regional Atmos. Environ., Institute of Urban Environment, Chinese Academy of Sciences, Xiamen, 361021, P. R. China
[4] State Key Laboratory of Environmental Criteria and Risk Assessment, Chinese Research Academy of Environmental Sciences, Beijing 100012, P. R. China
[5] Air Quality Research Division, Environment and Climate Change Canada, Toronto, Ontario M3H5T4, Canada
[6] College of Architecture and Environment, Sichuan University, Chengdu, P. R. China

Correspondence to: Weigang Wang (wangwg@iccas.ac.cn)

Abstract. Environmental temperature plays a vital role in controlling chemical transformations that lead to the formation of secondary organic aerosol (SOA), and ultimately impact composition and optical properties of the aerosol particles. In this study, we investigate optical properties of *n*-dodecane secondary organic aerosol under two temperature conditions: 5 ˚C and 25 ˚C. It is shown that low temperature can enhance the real part of refractive index (RI) of the SOA at the wavelengths of 532 nm and 375 nm. Mass spectrometry analysis reveals that molecular composition of *n*-dodecane SOA is significantly modified by temperature: a large amount of oligomers are formed under low temperature condition, which lead to higher RI values. These findings will help improve our understanding of the chemical composition and optical properties of SOA under different temperature conditions, and provide another possible explanation of the low visibility during winter.

1 Introduction

Organic aerosol, especially secondary organic aerosol (SOA), play a vital role in air quality, climate change, and human health (Kanakidou et al., 2005;Poschl, 2005;Mellouki et al., 2015;Poschl and Shiraiwa, 2015;von Schneidemesser et al., 2015;Shrivastava et al., 2017). SOA account for a high proportion of atmospheric particulate matter around the world, especially in the heavy polluted areas (Liu et al., 2017;Sun et al., 2014;Huang et al., 2014). Due to the variety of precursors and oxidation pathways, the composition of SOA is very complicated and variable (Lu, 2018;von Schneidemesser et al., 2015;Poschl and Shiraiwa, 2015;Hallquist et al., 2009;George et al., 2015), and the optical properties of SOA also exhibit different characteristics (Shrivastava et al., 2017;Zhang et al., 2015;Moise et al., 2015;Laskin et al., 2015). The complex

https://doi.org/10.5194/acp-2019-1218
Preprint. Discussion started: 13 February 2020

Atmospheric Chemistry and Physics Discussions

refractive index (RI), m= n + ki (n is the real part, and k is the imaginary part; they express the extent of scattering and absorbing, respectively), is the only intrinsic optical property of a particle. RI is controlled by the chemical composition and physical characteristics (e.g., morphology and shape) of a particle (Moise et al., 2015). Quantifying the RI of aerosol particles is highly important to evaluate their optical properties, and further estimate their impacts on atmospheric visibility and Earth's radiative balance.

Aerosol physicochemical properties are strongly dependent on the atmospheric conditions, e.g., relative humidity (Bateman et al., 2012;Sun et al., 2014), temperature (Wang et al., 2017), and oxidizing conditions (oxidant type, e.g., NO_3, OH, O_3; oxidation concentrations, e.g., photochemical age) (Cheng et al., 2016;Shrivastava et al., 2017;George et al., 2015;Kanakidou et al., 2005). Therefore, it is important to study the SOA formation and optical properties under varying atmospheric conditions to simulate the processes in the real atmosphere. There have been a number of smog chamber experiments on the effect of seed particles (Huang et al., 2017a;Denjean et al., 2014;Song et al., 2013;Lee et al., 2013;Li et al., 2018;Li et al., 2017a;Trainic et al., 2011), oxidant type (e.g., NO_3 (Peng et al., 2018;Lu et al., 2011), OH (Liu et al., 2015;Lin et al., 2015;Li et al., 2014;Nakayama et al., 2013;Cappa et al., 2011), and O_3 (Peng et al., 2018;Kim et al., 2014;Flores et al., 2014;Kim and Paulson, 2013)), oxidation concentrations (e.g., photochemical age (Zhong and Jang, 2014;Kim et al., 2014;Lambe et al., 2012;Lambe et al., 2013)), and relative humidity (RH) (Titos et al., 2016;McNeill, 2015;Denjean et al., 2015;Li et al., 2017b;Sareen et al., 2017;Ye et al., 2016;Michel Flores et al., 2012) on SOA formation and the RI values of SOA derived from both biogenic and anthropogenic volatile organic compounds (VOCs). However, studies covering the temperature effect on the SOA formation are relative limited (Takekawa et al., 2003;Svendby et al., 2008;Clark et al., 2016;Lamkaddam et al., 2016;Huang et al., 2017b;Qing Mu and Gerhard Lammel, 2018), and works on the effect of temperature on the SOA RI values are even rare (Kim et al., 2014). Field studies have shown that temperature is an important factor affecting rate constants of the oxidation process, vapor pressure of products, and SOA formation process and yields (Atkinson and Arey, 2003;Wang et al., 2017;Roy and Choi, 2017;Ding et al., 2017;Cui et al., 2016). Therefore, investigating temperature dependence is important to our better understanding of the formation, physical, and chemical properties of SOA under tropospheric conditions.

Long-chain alkanes, an important class of intermediate-volatility organic compounds (IVOCs) (Zhao et al., 2014) and a large fraction of diesel fuel and its exhaust (Gentner et al., 2012;Gentner et al., 2017), are important potential contributor of SOA (Presto et al., 2009;Zhao et al., 2016). Several previous studies have reported the formation of SOA derived from long chain alkanes under various conditions, including SOA compositions (Fahnestock et al., 2015;Hunter et al., 2014;Lim and Ziemann, 2005), SOA yields (Loza et al., 2014;Lim and Ziemann, 2009a), and the chemical mechanisms (Yee et al., 2012, 2013;Aimanant and Ziemann, 2013;Lim and Ziemann, 2009b). Recently, Lamkaddam et al. (2016) reported the temperature dependence of SOA formation from high NO_x photo-oxidaton of *n*-dodecane, and found that temperature did not significantly influence SOA yield. They attributed it to two possible reasons: the changes of reaction rate constants lead to different SOA composition; or the formed SOA are mainly non-volatile compounds that they are not sensitive to temperature. Wang et al. (2016) reported one additional chain-branching pathways of branched alkanes (2,5-dimethylhexane) in the low temperature

https://doi.org/10.5194/acp-2019-1218
Preprint. Discussion started: 13 February 2020

Atmospheric Chemistry and Physics Discussions

oxidation condition, and demonstrated that low temperature radical chain branching reactions are more complex than traditional conceptualized. Li et al. (2017a) reported the optical properties of SOA from *n*-dodecane, *n*-pentadecane, and *n*-heptadecane under various oxidation conditions under room temperature. However, knowledge about the effect of temperature on the chemical composition and optical properties of *n*-dodecane SOA in the absence of NO_x is still lacking, which limits our understanding of the role of SOA in visibility and radiative balance under different temperatures (e.g., in winter and summer).

In the present study, we determined the temperature effects on chemical composition and optical properties of SOA generated in a smog chamber during photo-oxidation of *n*-dodecane under low-NO_x condition. The results here will improve our understanding of the role of temperature in SOA chemical compositions and optical properties, and further the influence on air quality and radiative forcing.

2. Materials and methods

2.1 Smog Chamber Experiments

The experiments were performed in a dual-reactor smog chamber, the details of which were given previously (Wang et al., 2015). Briefly, multiple light sources were used in the chamber, with center wavelength of 365 nm (GE, F40BL), 340 nm (Q-lab, UVA-340), and 254 nm (PHILIPS, G36 T8). The RH and temperature in the chamber were continuously monitored and controlled during the whole experiments. The experiments were conducted under < 5% RH and under two temperatures: 25 ˚C (room temperature condition, R) and 5 ˚C (low temperature condition, L). The temperature fluctuation was ±0.5 ˚C for either condition. The *n*-dodecane (≥99%, Sigma-Aldrich) was photo-oxidized under low-NOx condition, with hydrogen peroxide (30% wt/wt, Beijing Chemical Works) as the OH precursor. *n*-Dodecane was added into the chamber first, followed by adding hydrogen peroxide. After that, wind turbine was turned on for 20 min to make sure that the materials in the chamber were well mixed.

When all the substances were added in the chamber, the chamber was set to the desired temperature. After the temperature was stabilized, the instruments outside the chamber were connected. The lights in the chamber were then turned on, and the photo-oxidation reaction started. The initial conditions for these experiments are listed in Table 1.

2.2 Measurements

All instruments were located within one meter of the chamber, and all the connection tubes were wrapped by insulation cotton to minimize the influence of room temperature. The concentration of NOx and formed O_3 in the smog chamber were monitored by the gas analyzers (Teledyne Advanced Pollution Instrumentation, Model T400 and Model T200UP, respectively). The concentration of *n*-dodecane was monitored by a proton transfer reaction quadrupole mass spectrometry (PTR-QMS 500, Ionicon). The NO^+ ion source of PTR-QMS was used when detecting the *n*-dodecane (Koss et al., 2016;Shi et al., 2019b;Shi et al., 2019a) .

https://doi.org/10.5194/acp-2019-1218
Preprint. Discussion started: 13 February 2020


Atmospheric Chemistry and Physics Discussions

The particle size distribution and density were detected by a scanning mobility particle sizer (SMPS, TSI) and a centrifugal particle mass analyzer (CPMA, Cambustion). A custom-made cavity ring-down spectrometer (CRDS) (Wang et al., 2012) was applied to monitor the optical property of the formed particles at 532 nm. A photoacoustic extinctiometer (PAX-375, Droplet Measurement Technologies) was used to measure the scattering, absorption, and extinction coefficients of formed SOA at 375 nm.

The formed aerosol particles were collected on the PTFE membrane with a pore size of 200 nm, and the membrane was dissolved with 5 mL methanol (99.9%, Fisher Chemical). The dissolved solution was analyzed with a UV−Vis light spectrometer (Avantes 2048F), which was used to detect the absorbing property (to derive the imaginary part of RI, k) at 532 nm. The solution was also analyzed with electrospray ionization time-of-flight mass spectrometry (ESI-TOF-MS, Bruker, Impact HD) to obtain the chemical composition of the formed SOA. Positive ion mode was used for the ESI-TOF-MS. The absolute mass error was below 3 ppm, and the typical mass resolving power is ＞30000 at m/z 200.

2.3 Calculation Method of RI Values

The RI values of the particles formed in the smog chamber was estimated based on both the extinction and scattering coefficients and Mie-Lorenz theory (Bohren, 1983). The details of the calculation method of RI values are given in the Supporting Information and also in our previous publications (Wang et al., 2012;Phillips and Smith, 2014;Li et al., 2017a;Li et al., 2017b;Li et al., 2018;Peng et al., 2018).

Briefly, the extinction coefficients (α_{ext}) of the particles with CRDS can be calculated with Eq.(1):

$$\alpha_{ext} = \frac{L}{cl}\left(\frac{1}{\tau} - \frac{1}{\tau_0}\right) \quad (1)$$

where L is the distance of the two mirrors in the cavity, l is the length of the cavity that filled with aerosol particles, c is the speed of the light, τ_0 is the ring down time of the CRDS when it is filled with zero air, and τ is the ting down time of the CRDS when it is filled with aerosol particles

For the particles formed in the smog chamber, the extinction efficiency (Q_{ext}) can be expressed as Eq.(2):

$$Q_{ext}(D_s) = \frac{4\alpha_{ext}}{S_{tot}} \quad (2)$$

where S_{tot} is the total surface area of the particles, and Ds is the surface mean diameter, which can be obtained with SMPS.

The uncertainties of the particle concentration and surface mean diameter measured by SMPS are ± 10% and ± 1% respectively. The uncertainty of the retrieval method is ± 0.002, and the uncertainty of the measured extinction coefficient with CRDS is ± 3%, resulting in the final uncertainty of the retrieved RI value to be about 0.02–0.03.

The RI values of the products in SOA are predicted with the quantitative structure–property relationship (QSPR), which is based on the molecular formula (Redmond and Thompson, 2011). The details can be found in the Supporting Information.

https://doi.org/10.5194/acp-2019-1218
Preprint. Discussion started: 13 February 2020

Atmospheric Chemistry and Physics Discussions

2.4 Impact of Temperature on Direct Radiative Forcing

The simple forcing efficiency (SFE) is used to dertermine the relative importance of optical properties of the aerosol to direct radiative forcing at the Earth's surface (Bond and Bergstrom, 2006):

$$SFE = \frac{S_0}{4}\tau_{atm}^2(1-F_c)[2(1-a_s)^2\frac{Q_{bs}C}{M} - 4a_s\frac{Q_aC}{M}] \quad (3)$$

where S_0 is the solar radiation, τ_{atm} is the transmission of the atmosphere, F_c is the cloud fraction, a_s is the surface albedo, Q_{bs} and Q_a are the backscattering and absorption efficiency of the aerosol particles, M is the aerosol mass, and C is the cross section of the aerosol.

The SOA derived from *n*-dodecane have negligible absorption at the wavelengths of 532 nm and 375 nm under the two temperature conditions, so the value of Q_a is zero, and the impact of temperature on the direct radiative forcing (DRF) can be expressed with Eq. (4), and this will be discussed Section. 3.5.

$$DRF\ ratio = \frac{SFE_{low\ temperature}}{SFE_{normal\ temperature}} = \frac{Q_{bs,low\ tem.}}{Q_{bs,normal\ tem.}} \quad (4)$$

3. Results and Discussion

3.1 Photo-oxidation Experiments

The profiles of the *n*-dodecane photo-oxidation experiments at different temperatures are shown in Figure S1. As similar amount of n-dodecane and oxidant were added to the smog chamber and the reaction rate is lower under low temperature, the reaction time of low temperature condition is significantly longer than the room temperature condition: 4 to 5 h for room temperature, and 8 to 9 h for low temperature. Under room temperature condition, the total surface concentrstion and mass reach a maximum after 3 h; while for low temperature condition, this time is 6 h.

3.2 Effect of Temperature on RI Values

Optical properties of the formed particles are analyzed after the mass concentration of the aerosol reaches the maximum, and the last 1 h data are used. During this period, the optical properties of the particles tend to be stable and will not change much. The SOA derived from n-dodecane have no significant absorption both at 532 nm and 375 nm, similar to our previous study,(Li et al., 2017a) and the imaginary part of RI will not be discussed here. The real part of RI obtained in this study is shown in Figure 1. As shown in Figure 1, the RI values at 532 nm under room temperature are similar to our previous study,(Li et al., 2017a) while the two temperature conditions have significantly different ranges for RI: 1.472-1.486 (25 ˚C) and 1.502-1.526 (5 ˚C) at 532 nm; 1.51-1.53 (25 ˚C) and 1.532-1.56 (5 ˚C) at 375 nm. The various RI values at different temperature indicate that lower reaction temperature (from 25 ˚C to 5 ˚C) has a substantial enhance effect (~0.03 at 532 nm, ~0.02 at 375 nm) on the RI of *n*-dodecane SOA. The mass spectrometry analysis below (Section 3.3) is applied to obtain chemical composition information and explain the phenomenon above.

https://doi.org/10.5194/acp-2019-1218
Preprint. Discussion started: 13 February 2020


Atmospheric Chemistry and Physics Discussions

3.3 Temperature Effect on Chemical Composition and Reaction Mechanism

The higher RI values under low temperature indicate that the temperature may change the chemical composition of SOA by changing the reaction types or shifting the balance of different pathways. The mass spectra (MS) of *n*-dodecane SOA obtained by ESI-TOF-MS in positive ion mode are shown in Figure 2, which provides the molecular insight into the chemical changes under different temperature conditions. We identified about 260 individual masses for SOA under two temperature conditions, and the details are shown in Figure S2 and Table S1. The spectrum under low temperature is significantly different with the spectrum under room temperature, with large amount of ions corresponding to monomer, dimer, trimer, and tetramer. This suggests that oligomerization may play a dominant role under low temperature condition.

The molecular composition of *n*-dodecane SOA was significantly modified by temperature conditions, with the averaging SOA formula changing from $C_{14.98}H_{26.47}O_{5.53}$ (R) to $C_{21.25}H_{40.44}O_{7.43}$ (L). The average carbon number increases from 14.98 at room temperature to 21.25 at low temperature, indicating that the SOA molecules are larger at low temperature. The average O/C and H/C ratios at room temperature condition are 0.37 and 1.72, respectively, while at low temperature condition the ratios are 0.35 and 1.90, respectively. The products formed under low temperature tend to have higher H/C ratio and lower O/C ratio compared with the products under room temperature. The details of the O/C and H/C ratios of the products formed at different temperature conditions can be referred to Figure 3a. The phenomenon above may be due to the presence of oligomers.

One possible explanation is that low temperature condition promotes gas-particle partitioning and changes the particle phase reaction. The gas-phase OH oxidation can reduce H/C and increase O/C ratios (Heald et al., 2010;Lambe et al., 2015;Li et al., 2018), while particle-phase oligomerization almost won't change O/C and H/C ratios (Charron et al., 2019). Under high temperature condition, more gas-phase oxidation steps are needed to produce the less volatile products to condense into particle-phase (because of the high temperature, i.e., high saturation vapor pressure). Hence, products formed under high temperature have lower H/C and higher O/C ratios. In contrast, the more volatile (i.e., less oxidized) products are readily to condense into particle phase under low temperature, and then undergo particle phase reactions, e.g., oligomerization, leading to the formation of products with higher H/C and lower O/C ratios. This phenomenon is consistent with Kim et al. (2014), they studied the dependence of real part of RI on O/C and H/C ratios of SOA derived from limonene and α-pinene, and found that the higher percentage of less oxygenated semivolatile substances were responsible for the higher RI values.

For particle-phase reactions, there are mainly two reaction pathways (Fahnestock et al., 2015;Yee et al., 2012, 2013): intramolecular cyclization of multifunctional hydroperoxides (form furan derivatives); intermolecular oligomerization of multifunctional hydroperoxides with aldehydes (form peroxyhemiacetal, PHA). The two pathways are competitive during the particle phase reaction process. According to the mass spectra analysis, we speculate that the low temperature promotes the progress of the oligomerization reaction, and makes it the primary pathway in the particle phase, as shown in Figure S3. As discussed above, the products with higher volatility and lower oxidation state will condense on the particle phase under low

https://doi.org/10.5194/acp-2019-1218
Preprint. Discussion started: 13 February 2020


Atmospheric Chemistry and Physics Discussions

temperature condition and then participate in the particle phase reaction, which will further promote the oligomerization reaction.

Another possible explanation is that the pathway of the gas phase reaction changes under low temperature condition comparing with room temperature condition. Wang et al. (2016) reported that highly oxidized multifunctional molecules have been detected during the gas-phase low temperature oxidation of 2,5-dimethylhexane. Combining existing mass spectrometry information and related reference, we speculate that under low temperature condition the oligomers may also be formed by gas phase radical oligomerization and then rapidly deposit into the particle phase. However, these are speculations based on the existing analysis results. The specific reaction mechanism under low temperature condition needs further investigation.

3.4 Relationship between RI Values and Chemical Composition of SOA

Refractive index of aerosol particles is fundamentally the results of a combination of particle chemical compositions and internal mixing. SOA particles formed in the smog chamber are treated as homogenous mixtures, and the RI values of which can be expressed as (Redmond and Thompson, 2011):

$$RI = \sum x_i RI_i \quad (5)$$

where x_i is the fraction of the i_{th} component, and RI_i is the refractive index of component i.

The RI values are calculated for the identified products (with high intensity) under room and low temperature conditions, and the details are shown in Figure 3b and Table S1. It can be clearly seen that the RI values of the products at room temperature condition are mainly in the range of 1.4 to 1.5, and the degree of oligomerization is mainly in the range of monomer and dimerization. However, for the products under low temperature condition, the RI value is in the range of 1.4 to 1.55, and the degree of oligomers can reach tetramerization. As the degree of oligomerization increases, RI is gradually increasing as well. This generally explains the higher RI of SOA under lower temperature condition.

To further validate our speculation and identify the relationship between the measured RI values and the chemical composition of *n*-dodecane SOA, we choose a surrogate system containing 11 PHA oligomerization and 2 cyclization reactions (with different degree of unsaturation and functional groups) to calculate the expected RI values using the quantitative structure−property relationship (QSPR) method based on the molecular formula and structure (Redmond and Thompson, 2011). The details of the 13 reactions and related molecular information are shown in Figure S4 and Table S2, while the relationship between the predicted RI values with the degree of unsaturation, and the degree of oligomerization are shown in Figure S5. Strong correlations are observed between predicted RI values and unsaturation, and the degree of oligomerization. With the same unsaturation, the RI values will increase with the increasing degree of oligomerization; under the same degree oligomerization, the RI values will increase with the increasing degree of unsaturation. In addition, the RI values of the surrogate system are similar with the identified substances, which further confirm the effect of oligomers on RI values.

https://doi.org/10.5194/acp-2019-1218
Preprint. Discussion started: 13 February 2020


Atmospheric Chemistry and Physics Discussions

3.5 Atmospheric and Climate Implications

Figure 4 shows the ratios of light extinction efficiency (Q_{ext}) and direct radiative forcing (DRF) of *n*-dodecane SOA under different temperature conditions, from which we can know the impacts of temperature on the role of *n*-dodecane SOA in visibility and radiative balance. As shown in Figure 4a and 4c, the extinction efficiency (Q_{ext}) of SOA generated under low temperature is larger than SOA generated under room temperature in the size range of 50 to 200 nm, the range of which are the most atmospherically relevant (Zhang et al., 2015;Guo et al., 2014). The enhancement is about 7%-20% at 532 nm, and about 1%-21% at 375 nm. This suggests that the extinction efficiency (Q_{ext}) of SOA formed from *n*-dodecane (perhaps other long-chain alkanes in general) is higher in winter than in summer, which will result in lower visibility.

According to field observations, haze occurs more frequently in winter, especially in China (Cheng et al., 2016;Huang et al., 2014;Guo et al., 2014;Parrish et al., 2007). The enhancement in light extinction of SOA and polymer composition formed under low temperature condition provides one possible explanation for the low visibility of winter haze. It has also been reported that UV-scattering particles in the boundary layer can accelerate photochemical reactions and haze production (Sun et al., 2014). The observations above show that the scattering property of formed SOA increases under low temperature condition, which may be another possible reason for the rapid occurrence of haze in winter.

As shown in Figure 4b and d, the DRF under low temperature condition is generally larger than room temperature condition: the enhancement is about 6%-19% at 532 nm (50-200 nm), and about 7%-22% at 375 nm (50-180 nm); while for the size range of 180-200 nm, low temperature decreases the DRF ratio about 3% at 375 nm. This phenomenon implies that the SOA generated in winter (low temperature) may have larger DRF on the Earth's surface than the SOA generated in summer (room temperature). It may also imply that the temperature condition should be considered when evaluating the DRF of the aerosol particles generated in the atmosphere.

4 Conclusions

To the best of our knowledge, this is the first report about optical properties of long-chain alkane SOA at low temperature condition. The modification in temperature significantly changes the chemical composition of the particulate phase. From the oligomer component at low temperature condition, it is presumed that the oligomerization is dominant at low temperature. The presence of oligomers in the SOA particles results in an increase of RI values. This study will help to improve our understanding of the lower visibility and the formation of haze in winter. Our results also show the need for further investigation on the atmospheric parameters influencing SOA formation and optical properties.

Author contributions. WW conceived and led the studies. JL,WZ and CP performed chamber simulation and data analysis. KL, LZ, BS, YC, ML, HL and MG discussed the results and commented on the manuscript. JL prepared the manuscript with contributions from all co-authors.

https://doi.org/10.5194/acp-2019-1218
Preprint. Discussion started: 13 February 2020

Atmospheric Chemistry and Physics Discussions

Data availability. The data used in this study are available upon request from the corresponding author.

Competing interests. The authors declare that they have no conflict of interest.

Acknowledgements

This project was supported by the National Key Research and Development Program of China (2017YFC0209506) and National Natural Science Foundation of China (41822703, 91744204, 91844301).

References

Aimanant, S., and Ziemann, P. J.: Chemical Mechanisms of Aging of Aerosol Formed from the Reaction of n-Pentadecane with OH Radicals in the Presence of NOx, Aerosol Science and Technology, 47, 979-990, 10.1080/02786826.2013.804621, 2013.

Atkinson, R., and Arey, J.: Atmospheric degradation of volatile organic compounds, Chem. Rev., 103, 4605-4638, 10.1021/cr0206420, 2003.

Bateman, A. P., Laskin, J., Laskin, A., and Nizkorodov, S. A.: Applications of high-resolution electrospray ionization mass spectrometry to measurements of average oxygen to carbon ratios in secondary organic aerosols, Environmental science & technology, 46, 8315-8324, 10.1021/es3017254, 2012.

Bohren, C. F. H., D. R.: Absorption and Scattering of Light by Small Particles, 1983.

Bond, T. C., and Bergstrom, R. W.: Light Absorption by Carbonaceous Particles: An Investigative Review, Aerosol Science and Technology, 40, 27-67, 10.1080/02786820500421521, 2006.

Cappa, C. D., Che, D. L., Kessler, S. H., Kroll, J. H., and Wilson, K. R.: Variations in organic aerosol optical and hygroscopic properties upon heterogeneous OH oxidation, Journal of Geophysical Research, 116, 10.1029/2011jd015918, 2011.

Charron, A., Polo-Rehn, L., Besombes, J.-L., Golly, B., Buisson, C., Chanut, H., Marchand, N., Guillaud, G., and Jaffrezo, J.-L.: Identification and quantification of particulate tracers of exhaust and non-exhaust vehicle emissions, Atmospheric Chemistry and Physics, 19, 5187-5207, 10.5194/acp-19-5187-2019, 2019.

Cheng, Y., Zheng, G., Wei, C., Mu, Q., Zheng, B., Wang, Z., Gao, M., Zhang, Q., He, K., Carmichael, G., Poschl, U., and Su, H.: Reactive nitrogen chemistry in aerosol water as a source of sulfate during haze events in China, Science advances, 2, e1601530-e1601530, 10.1126/sciadv.1601530, 2016.

Clark, C. H., Kacarab, M., Nakao, S., Asa-Awuku, A., Sato, K., and Cocker, D. R., 3rd: Temperature Effects on Secondary Organic Aerosol (SOA) from the Dark Ozonolysis and Photo-Oxidation of Isoprene, Environmental science & technology, 10.1021/acs.est.5b05524, 2016.

Cui, L., Zhang, Z., Huang, Y., Lee, S. C., Blake, D. R., Ho, K. F., Wang, B., Gao, Y., Wang, X. M., and Louie, P. K. K.: Measuring OVOCs and VOCs by PTR-MS in an urban roadside microenvironment of Hong Kong: relative humidity and temperature dependence, and field intercomparisons, Atmospheric Measurement Techniques, 9, 5763-5779, 10.5194/amt-9-5763-2016, 2016.

Denjean, C., Formenti, P., Picquet-Varrault, B., Katrib, Y., Pangui, E., Zapf, P., and Doussin, J. F.: A new experimental approach to study the hygroscopic and optical properties of aerosols: application to ammonium sulfate particles, Atmospheric Measurement Techniques, 7, 183-197, 10.5194/amt-7-183-2014, 2014.

Denjean, C., Formenti, P., Picquet-Varrault, B., Pangui, E., Zapf, P., Katrib, Y., Giorio, C., Tapparo, A., Monod, A., Temime-Roussel, B., Decorse, P., Mangeney, C., and Doussin, J. F.: Relating hygroscopicity and optical properties to chemical composition and structure of secondary organic aerosol particles generated from the ozonolysis of α-pinene, Atmospheric

https://doi.org/10.5194/acp-2019-1218
Preprint. Discussion started: 13 February 2020

Chemistry and Physics, 15, 3339-3358, 10.5194/acp-15-3339-2015, 2015.
Ding, X., Zhang, Y. Q., He, Q. F., Yu, Q. Q., Wang, J. Q., Shen, R. Q., Song, W., Wang, Y. S., and Wang, X. M.: Significant Increase of Aromatics-Derived Secondary Organic Aerosol during Fall to Winter in China, Environmental science & technology, 51, 7432-7441, 10.1021/acs.est.6b06408, 2017.
Fahnestock, K. A. S., Yee, L. D., Loza, C. L., Coggon, M. M., Schwantes, R., Zhang, X., Dalleska, N. F., and Seinfeld, J. H.: Secondary Organic Aerosol Composition from C-12 Alkanes, J. Phys. Chem. A, 119, 4281-4297, 10.1021/jp501779w, 2015.
Flores, J. M., Washenfelder, R. A., Adler, G., Lee, H. J., Segev, L., Laskin, J., Laskin, A., Nizkorodov, S. A., Brown, S. S., and Rudich, Y.: Complex refractive indices in the near-ultraviolet spectral region of biogenic secondary organic aerosol aged with ammonia, Physical Chemistry Chemical Physics, 16, 10629-10642, 10.1039/c4cp01009d, 2014.
Gentner, D. R., Isaacman, G., Worton, D. R., Chan, A. W. H., Dallmann, T. R., Davis, L., Liu, S., Day, D. A., Russell, L. M., Wilson, K. R., Weber, R., Guha, A., Harley, R. A., and Goldstein, A. H.: Elucidating secondary organic aerosol from diesel and gasoline vehicles through detailed characterization of organic carbon emissions, Proceedings of the National Academy of Sciences of the United States of America, 109, 18318-18323, 10.1073/pnas.1212272109, 2012.
Gentner, D. R., Jathar, S. H., Gordon, T. D., Bahreini, R., Day, D. A., El Haddad, I., Hayes, P. L., Pieber, S. M., Platt, S. M., de Gouw, J., Goldstein, A. H., Harley, R. A., Jimenez, J. L., Prévôt, A. S. H., and Robinson, A. L.: Review of Urban Secondary Organic Aerosol Formation from Gasoline and Diesel Motor Vehicle Emissions, Environmental science & technology, 51, 1074-1093, 10.1021/acs.est.6b04509, 2017.
George, C., Ammann, M., DAnna, B., Donaldson, D. J., and Nizkorodov, S. A.: Heterogeneous photochemistry in the atmosphere, Chemical reviews, 115, 4218-4258, 10.1021/cr500648z, 2015.
Guo, S., Hu, M., Zamora, M. L., Peng, J., Shang, D., Zheng, J., Du, Z., Wu, Z., Shao, M., Zeng, L., Molina, M. J., and Zhang, R.: Elucidating severe urban haze formation in China, Proc Natl Acad Sci U S A, 111, 17373-17378, 10.1073/pnas.1419604111, 2014.
Hallquist, M., Wenger, J. C., Baltensperger, U., Rudich, Y., Simpson, D., Claeys, M., Dommen, J., Donahue, N. M., George, C., Goldstein, A. H., Hamilton, J. F., Herrmann, H., Hoffmann, T., Iinuma, Y., Jang, M., Jenkin, M. E., Jimenez, J. L., Kiendler-Scharr, A., Maenhaut, W., McFiggans, G., Mentel, T. F., Monod, A., Prevot, A. S. H., Seinfeld, J. H., Surratt, J. D., Szmigielski, R., and Wildt, J.: The formation, properties and impact of secondary organic aerosol: current and emerging issues, Atmospheric Chemistry and Physics, 9, 5155-5236, 2009.
Heald, C. L., Kroll, J. H., Jimenez, J. L., Docherty, K. S., DeCarlo, P. F., Aiken, A. C., Chen, Q., Martin, S. T., Farmer, D. K., and Artaxo, P.: A simplified description of the evolution of organic aerosol composition in the atmosphere, Geophysical Research Letters, 37, 10.1029/2010gl042737, 2010.
Huang, M., Hao, L., Cai, S., Gu, X., Zhang, W., Hu, C., Wang, Z., Fang, L., and Zhang, W.: Effects of inorganic seed aerosols on the particulate products of aged 1,3,5-trimethylbenzene secondary organic aerosol, Atmospheric Environment, 152, 490-502, 10.1016/j.atmosenv.2017.01.010, 2017a.
Huang, R. J., Zhang, Y., Bozzetti, C., Ho, K. F., Cao, J. J., Han, Y., Daellenbach, K. R., Slowik, J. G., Platt, S. M., Canonaco, F., Zotter, P., Wolf, R., Pieber, S. M., Bruns, E. A., Crippa, M., Ciarelli, G., Piazzalunga, A., Schwikowski, M., Abbaszade, G., Schnelle-Kreis, J., Zimmermann, R., An, Z., Szidat, S., Baltensperger, U., El Haddad, I., and Prevot, A. S.: High secondary aerosol contribution to particulate pollution during haze events in China, Nature, 514, 218-222, 10.1038/nature13774, 2014.
Huang, W., Saathoff, H., Pajunoja, A., Shen, X., Naumann, K.-H., Wagner, R., Virtanen, A., Leisner, T., and Mohr, C.: α-pinene secondary organic aerosol at low temperature: Chemical composition and implications for particle viscosity, Atmospheric Chemistry and Physics Discussions, 1-23, 10.5194/acp-2017-793, 2017b.
Hunter, J. F., Carrasquillo, A. J., Daumit, K. E., and Kroll, J. H.: Secondary organic aerosol formation from acyclic, monocyclic, and polycyclic alkanes, Environmental science & technology, 48, 10227-10234, 10.1021/es502674s, 2014.
Kanakidou, M., Seinfeld, J. H., Pandis, S. N., Barnes, I., Dentener, F. J., Facchini, M. C., Van Dingenen, R., Ervens, B., Nenes, A., Nielsen, C. J., Swietlicki, E., Putaud, J. P., Balkanski, Y., Fuzzi, S., Horth, J., Moortgat, G. K., Winterhalter, R., Myhre, C. E. L., Tsigaridis, K., Vignati, E., Stephanou, E. G., and Wilson, J.: Organic aerosol and global climate modelling: a review, Atmospheric Chemistry and Physics, 5, 1053-1123, 2005.
Kim, H., and Paulson, S. E.: Real refractive indices and volatility of secondary organic aerosol generated from photooxidation and ozonolysis of limonene, α-pinene and toluene, Atmospheric Chemistry and Physics, 13, 7711-7723, 10.5194/acp-13-7711-2013, 2013.
Kim, H., Liu, S., Russell, L. M., and Paulson, S. E.: Dependence of Real Refractive Indices on O:C, H:C and Mass Fragments

https://doi.org/10.5194/acp-2019-1218
Preprint. Discussion started: 13 February 2020

of Secondary Organic Aerosol Generated from Ozonolysis and Photooxidation of Limonene and alpha-Pinene, Aerosol Science and Technology, 48, 498-507, 10.1080/02786826.2014.893278, 2014.

Koss, A. R., Warneke, C., Yuan, B., Coggon, M. M., Veres, P. R., and de Gouw, J. A.: Evaluation of NO+ reagent ion chemistry for online measurements of atmospheric volatile organic compounds, Atmospheric Measurement Techniques, 9, 2909-2925, 10.5194/amt-9-2909-2016, 2016.

Lambe, A. T., Onasch, T. B., Croasdale, D. R., Wright, J. P., Martin, A. T., Franklin, J. P., Massoli, P., Kroll, J. H., Canagaratna, M. R., Brune, W. H., Worsnop, D. R., and Davidovits, P.: Transitions from functionalization to fragmentation reactions of laboratory secondary organic aerosol (SOA) generated from the OH oxidation of alkane precursors, Environmental science & technology, 46, 5430-5437, 10.1021/es300274t, 2012.

Lambe, A. T., Cappa, C. D., Massoli, P., Onasch, T. B., Forestieri, S. D., Martin, A. T., Cummings, M. J., Croasdale, D. R., Brune, W. H., Worsnop, D. R., and Davidovits, P.: Relationship between Oxidation Level and Optical Properties of Secondary Organic Aerosol, Environmental science & technology, 47, 6349-6357, 10.1021/es401043j, 2013.

Lambe, A. T., Chhabra, P. S., Onasch, T. B., Brune, W. H., Hunter, J. F., Kroll, J. H., Cummings, M. J., Brogan, J. F., Parmar, Y., Worsnop, D. R., Kolb, C. E., and Davidovits, P.: Effect of oxidant concentration, exposure time, and seed particles on secondary organic aerosol chemical composition and yield, Atmospheric Chemistry and Physics, 15, 3063-3075, 10.5194/acp-15-3063-2015, 2015.

Lamkaddam, H., Gratien, A., Pangui, E., Cazaunau, M., Picquet-Varrault, B., and Doussin, J.-F.: High-NOx Photooxidation of n-Dodecane: Temperature Dependence of SOA Formation, Environmental science & technology, 10.1021/acs.est.6b03821, 2016.

Laskin, A., Laskin, J., and Nizkorodov, S. A.: Chemistry of atmospheric brown carbon, Chemical reviews, 115, 4335-4382, 10.1021/cr5006167, 2015.

Lee, A. K. Y., Zhao, R., Li, R., Liggio, J., Li, S.-M., and Abbatt, J. P. D.: Formation of Light Absorbing Organo-Nitrogen Species from Evaporation of Droplets Containing Glyoxal and Ammonium Sulfate, Environmental Science & Technology, 47, 12819-12826, 10.1021/es402687w, 2013.

Li, J., Li, K., Wang, W., Wang, J., Peng, C., and Ge, M.: Optical properties of secondary organic aerosols derived from long-chain alkanes under various NO x and seed conditions, Science of The Total Environment, 579, 1699-1705, 10.1016/j.scitotenv.2016.11.189, 2017a.

Li, K., Wang, W., Ge, M., Li, J., and Wang, D.: Optical properties of secondary organic aerosols generated by photooxidation of aromatic hydrocarbons, Scientific Reports, 4, 4922-4922, 10.1038/srep04922, 2014.

Li, K., Li, J., Liggio, J., Wang, W., Ge, M., Liu, Q., Guo, Y., Tong, S., Li, J., Peng, C., Jing, B., Wang, D., and Fu, P.: Enhanced Light Scattering of Secondary Organic Aerosols by Multiphase Reactions, Environmental science & technology, 10.1021/acs.est.6b03229, 2017b.

Li, K., Li, J., Wang, W., Li, J., Peng, C., Wang, D., and Ge, M.: Effects of Gas-Particle Partitioning on Refractive Index and Chemical Composition of m-Xylene Secondary Organic Aerosol, J Phys Chem A, 10.1021/acs.jpca.7b12792, 2018.

Lim, Y. B., and Ziemann, P. J.: Products and mechanism of secondary organic aerosol formation from reactions of n-alkanes with OH radicals in the presence of NOx, Environmental science & technology, 39, 9229-9236, 10.1021/es051447g, 2005.

Lim, Y. B., and Ziemann, P. J.: Effects of Molecular Structure on Aerosol Yields from OH Radical-Initiated Reactions of Linear, Branched, and Cyclic Alkanes in the Presence of NOx, Environmental science & technology, 43, 2328-2334, 10.1021/es803389s, 2009a.

Lim, Y. B., and Ziemann, P. J.: Chemistry of Secondary Organic Aerosol Formation from OH Radical-Initiated Reactions of Linear, Branched, and Cyclic Alkanes in the Presence of NOx, Aerosol Science and Technology, 43, 604-619, 10.1080/02786820902802567, 2009b.

Lin, P., Liu, J., Shilling, J. E., Kathmann, S. M., Laskin, J., and Laskin, A.: Molecular characterization of brown carbon (BrC) chromophores in secondary organic aerosol generated from photo-oxidation of toluene, Physical Chemistry Chemical Physics, 17, 23312-23325, 10.1039/c5cp02563j, 2015.

Liu, H., Man, H., Cui, H., Wang, Y., Deng, F., Wang, Y., Yang, X., Xiao, Q., Zhang, Q., Ding, Y., and He, K.: An updated emission inventory of vehicular VOCs and IVOCs in China, Atmospheric Chemistry and Physics, 17, 12709-12724, 10.5194/acp-17-12709-2017, 2017.

Liu, P. F., Abdelmalki, N., Hung, H. M., Wang, Y., Brune, W. H., and Martin, S. T.: Ultraviolet and visible complex refractive indices of secondary organic material produced by photooxidation of the aromatic compounds toluene and m-xylene,

Atmospheric Chemistry and Physics, 15, 1435-1446, 10.5194/acp-15-1435-2015, 2015.
Loza, C. L., Craven, J. S., Yee, L. D., Coggon, M. M., Schwantes, R. H., Shiraiwa, M., Zhang, X., Schilling, K. A., Ng, N. L., Canagaratna, M. R., Ziemann, P. J., Flagan, R. C., and Seinfeld, J. H.: Secondary organic aerosol yields of 12-carbon alkanes, Atmospheric Chemistry and Physics, 14, 1423-1439, 10.5194/acp-14-1423-2014, 2014.
Lu, J. W., Flores, J. M., Lavi, A., Abo-Riziq, A., and Rudich, Y.: Changes in the optical properties of benzo a pyrene-coated aerosols upon heterogeneous reactions with NO2 and NO3, Physical Chemistry Chemical Physics, 13, 6484-6492, 10.1039/c0cp02114h, 2011.
Lu, K., Guo, S., Tan, Z., Wang, H., Shang, D., Liu, Y., Li, X., Wu, Z., Hu, M., and Zhang, Y.: Exploring atmospheric free-radical chemistry in China: the self-cleansing capacity and the formation of secondary air pollution, National Science Review, 10.1093/nsr/nwy073, 2018.
McNeill, V. F.: Aqueous organic chemistry in the atmosphere: sources and chemical processing of organic aerosols, Environmental science & technology, 49, 1237-1244, 10.1021/es5043707, 2015.
Mellouki, A., Wallington, T. J., and Chen, J.: Atmospheric chemistry of oxygenated volatile organic compounds: impacts on air quality and climate, Chemical reviews, 115, 3984-4014, 10.1021/cr500549n, 2015.
Michel Flores, J., Bar-Or, R. Z., Bluvshtein, N., Abo-Riziq, A., Kostinski, A., Borrmann, S., Koren, I., Koren, I., and Rudich, Y.: Absorbing aerosols at high relative humidity: linking hygroscopic growth to optical properties, Atmospheric Chemistry and Physics, 12, 5511-5521, 10.5194/acp-12-5511-2012, 2012.
Moise, T., Flores, J. M., and Rudich, Y.: Optical properties of secondary organic aerosols and their changes by chemical processes, Chemical reviews, 115, 4400-4439, 10.1021/cr5005259, 2015.
Nakayama, T., Sato, K., Matsumi, Y., Imamura, T., Yamazaki, A., and Uchiyama, A.: Wavelength and NOx dependent complex refractive index of SOAs generated from the photooxidation of toluene, Atmospheric Chemistry and Physics, 13, 531-545, 10.5194/acp-13-531-2013, 2013.
Parrish, D. D., Stohl, A., Forster, C., Atlas, E. L., Blake, D. R., Goldan, P. D., Kuster, W. C., and de Gouw, J. A.: Effects of mixing on evolution of hydrocarbon ratios in the troposphere, Journal of Geophysical Research-Atmospheres, 112, 10.1029/2006jd007583, 2007.
Peng, C., Wang, W., Li, K., Li, J., Zhou, L., Wang, L., and Ge, M.: The optical properties of limonene secondary organic aerosols: the role of NO3, OH and O3 in the oxidation processes, Journal of Geophysical Research: Atmospheres, 10.1002/2017jd028090, 2018.
Phillips, S. M., and Smith, G. D.: Light Absorption by Charge Transfer Complexes in Brown Carbon Aerosols, Environmental Science & Technology Letters, 1, 382-386, 10.1021/ez500263j, 2014.
Poschl, U.: Atmospheric aerosols: Composition, transformation, climate and health effects, Angewandte Chemie-International Edition, 44, 7520-7540, 10.1002/anie.200501122, 2005.
Poschl, U., and Shiraiwa, M.: Multiphase Chemistry at the Atmosphere-Biosphere Interface Influencing Climate and Public Health in the Anthropocene, Chem. Rev., 115, 4440-4475, 10.1021/cr500487s, 2015.
Presto, A. A., Miracolo, M. A., Kroll, J. H., Worsnop, D. R., Robinson, A. L., and Donahue, N. M.: Intermediate-Volatility Organic Compounds: A Potential Source of Ambient Oxidized Organic Aerosol, Environmental science & technology, 43, 4744-4749, 10.1021/es803219q, 2009.
Qing Mu, M. S., Mega Octaviani, Nan Ma, Aijun Ding, Hang Su,, and Gerhard Lammel, U. P., Yafang Cheng: Temperature effect on phase state and reactivity controls atmospheric multiphase chemistry and transport of PAHs, Science Advances, 4, 10.1126/sciadv.aap7314, 2018.
Redmond, H., and Thompson, J. E.: Evaluation of a quantitative structure-property relationship (QSPR) for predicting mid-visible refractive index of secondary organic aerosol (SOA), Physical chemistry chemical physics : PCCP, 13, 6872-6882, 10.1039/c0cp02270e, 2011.
Roy, A., and Choi, Y.: Effect of ambient temperature on species lumping for total organic gases in gasoline exhaust emissions, Atmospheric Environment, 152, 240-245, 10.1016/j.atmosenv.2016.11.057, 2017.
Sareen, N., Waxman, E. M., Turpin, B. J., Volkamer, R., and Carlton, A. G.: Potential of Aerosol Liquid Water to Facilitate Organic Aerosol Formation: Assessing Knowledge Gaps about Precursors and Partitioning, Environmental science & technology, 51, 3327-3335, 10.1021/acs.est.6b04540, 2017.
Shi, B., Wang, W., Zhou, L., Li, J., Wang, J., Chen, Y., Zhang, W., and Ge, M.: Kinetics and mechanisms of the gas-phase reactions of OH radicals with three C15 alkanes, Atmospheric Environment, 207, 75-81, 2019a.

Shi, B., Wang, W., Zhou, L., Sun, Z., Fan, C., Chen, Y., Zhang, W., Qiao, Y., Qiao, Y., and Ge, M.: Atmospheric oxidation of C10~14 n-alkanes initiated by Cl atoms: Kinetics and mechanism, Atmospheric Environment, accepted, https://doi.org/10.1016/j.atmosenv.2019.117166, 2019b.

Shrivastava, M., Cappa, C. D., Fan, J., Goldstein, A. H., Guenther, A. B., Jimenez, J. L., Kuang, C., Laskin, A., Martin, S. T., Ng, N. L., Petaja, T., Pierce, J. R., Rasch, P. J., Roldin, P., Seinfeld, J. H., Shilling, J., Smith, J. N., Thornton, J. A., Volkamer, R., Wang, J., Worsnop, D. R., Zaveri, R. A., Zelenyuk, A., and Zhang, Q.: Recent advances in understanding secondary organic aerosol: Implications for global climate forcing, Reviews of Geophysics, 55, 509-559, 10.1002/2016rg000540, 2017.

Song, C., Gyawali, M., Zaveri, R. A., Shilling, J. E., and Arnott, W. P.: Light absorption by secondary organic aerosol from alpha-pinene: Effects of oxidants, seed aerosol acidity, and relative humidity, Journal of Geophysical Research-Atmospheres, 118, NIL_306-NIL_314, 2013.

Sun, Y., Jiang, Q., Wang, Z., Fu, P., Li, J., Yang, T., and Yin, Y.: Investigation of the sources and evolution processes of severe haze pollution in Beijing in January 2013, Journal of Geophysical Research-Atmospheres, 119, 4380-4398, 10.1002/2014jd021641, 2014.

Svendby, T. M., Lazaridis, M., and Tørseth, K.: Temperature dependent secondary organic aerosol formation from terpenes and aromatics, Journal of Atmospheric Chemistry, 59, 25-46, 10.1007/s10874-007-9093-7, 2008.

Takekawa, H., Minoura, H., and Yamazaki, S.: Temperature dependence of secondary organic aerosol formation by photo-oxidation of hydrocarbons, Atmospheric Environment, 37, 3413-3424, 10.1016/s1352-2310(03)00359-5, 2003.

Titos, G., Cazorla, A., Zieger, P., Andrews, E., Lyamani, H., Granados-Muñoz, M. J., Olmo, F. J., and Alados-Arboledas, L.: Effect of hygroscopic growth on the aerosol light-scattering coefficient: A review of measurements, techniques and error sources, Atmospheric Environment, 141, 494-507, 10.1016/j.atmosenv.2016.07.021, 2016.

Trainic, M., Abo Riziq, A., Lavi, A., Flores, J. M., and Rudich, Y.: The optical, physical and chemical properties of the products of glyoxal uptake on ammonium sulfate seed aerosols, Atmospheric Chemistry and Physics, 11, 9697-9707, 10.5194/acp-11-9697-2011, 2011.

von Schneidemesser, E., Monks, P. S., Allan, J. D., Bruhwiler, L., Forster, P., Fowler, D., Lauer, A., Morgan, W. T., Paasonen, P., Righi, M., Sindelarova, K., and Sutton, M. A.: Chemistry and the Linkages between Air Quality and Climate Change, Chemical reviews, 115, 3856-3897, 10.1021/acs.chemrev.5b00089, 2015.

Wang, J. M., Jeong, C.-H., Zimmerman, N., Healy, R. M., Hilker, N., and Evans, G. J.: Real-World Emission of Particles from Vehicles: Volatility and the Effects of Ambient Temperature, Environmental science & technology, 10.1021/acs.est.6b05328, 2017.

Wang, L., Wang, W., and Ge, M.: Extinction efficiencies of mixed aerosols measured by aerosol cavity ring down spectrometry, Chinese Science Bulletin, 57, 2567-2573, 10.1007/s11434-012-5146-7, 2012.

Wang, W.-G., Li, K., Zhou, L., Ge, M.-F., Hou, S.-Q., Tong, S.-R., Mu, Y.-J., and Jia, L.: Evaluation and Application of Dual-Reactor Chamber for Studying Atmospheric Oxidation Processes and Mechanisms, Acta Physico-Chimica Sinica, 31, 1251-1259, 10.3866/pku.whxb201504161, 2015.

Wang, Z., Zhang, L., Moshammer, K., Popolan-Vaida, D. M., Shankar, V. S. B., Lucassen, A., Hemken, C., Taatjes, C. A., Leone, S. R., Kohse-Höinghaus, K., Hansen, N., Dagaut, P., and Sarathy, S. M.: Additional chain-branching pathways in the low-temperature oxidation of branched alkanes, Combustion and Flame, 164, 386-396, 10.1016/j.combustflame.2015.11.035, 2016.

Ye, Q., Robinson, E. S., Ding, X., Ye, P., Sullivan, R. C., and Donahue, N. M.: Mixing of secondary organic aerosols versus relative humidity, Proceedings of the National Academy of Sciences, 113, 12649-12654, 10.1073/pnas.1604536113, 2016.

Yee, L. D., Craven, J. S., Loza, C. L., Schilling, K. A., Ng, N. L., Canagaratna, M. R., Ziemann, P. J., Flagan, R. C., and Seinfeld, J. H.: Secondary organic aerosol formation from low-NO(x) photooxidation of dodecane: evolution of multigeneration gas-phase chemistry and aerosol composition, J Phys Chem A, 116, 6211-6230, 10.1021/jp211531h, 2012.

Yee, L. D., Craven, J. S., Loza, C. L., Schilling, K. A., Ng, N. L., Canagaratna, M. R., Ziemann, P. J., Flagan, R. C., and Seinfeld, J. H.: Effect of chemical structure on secondary organic aerosol formation from C12 alkanes, Atmospheric Chemistry and Physics, 13, 11121-11140, 10.5194/acp-13-11121-2013, 2013.

Zhang, R., Wang, G., Guo, S., Zamora, M. L., Ying, Q., Lin, Y., Wang, W., Hu, M., and Wang, Y.: Formation of urban fine particulate matter, Chemical reviews, 115, 3803-3855, 10.1021/acs.chemrev.5b00067, 2015.

Zhao, B., Wang, S., Donahue, N. M., Jathar, S. H., Huang, X., Wu, W., Hao, J., and Robinson, A. L.: Quantifying the effect of organic aerosol aging and intermediate-volatility emissions on regional-scale aerosol pollution in China, Sci Rep, 6, 28815,

https://doi.org/10.5194/acp-2019-1218
Preprint. Discussion started: 13 February 2020

Atmospheric Chemistry and Physics Discussions

10.1038/srep28815, 2016.
Zhao, Y., Hennigan, C. J., May, A. A., Tkacik, D. S., de Gouw, J. A., Gilman, J. B., Kuster, W. C., Borbon, A., and Robinson, A. L.: Intermediate-volatility organic compounds: a large source of secondary organic aerosol, Environmental science & technology, 48, 13743-13750, 10.1021/es5035188, 2014.
Zhong, M., and Jang, M.: Dynamic light absorption of biomass-burning organic carbon photochemically aged under natural sunlight, Atmospheric Chemistry and Physics, 14, 1517-1525, 10.5194/acp-14-1517-2014, 2014.

Table 1. The initial conditions of the smog-chamber experiments.

Experiments No.[a]	HC (ppb)	H_2O_2 (ppm)	NO_X (ppb)	RH (%)	Temperature (℃)
Dod-R-1	58	1.03	<1	<5	25
Dod-R-2	52	1.03	<1	<5	25
Dod-L-1	43	1.07	<1	<5	5
Dod-L-2	50	1.09	<1	<5	5

[a]Experimental conditions: *n*-Dodecane room temperature (Dod-R), *n*-Dodecane low temperature (Dod-L)

https://doi.org/10.5194/acp-2019-1218
Preprint. Discussion started: 13 February 2020

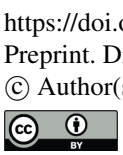

Atmospheric Chemistry and Physics Discussions

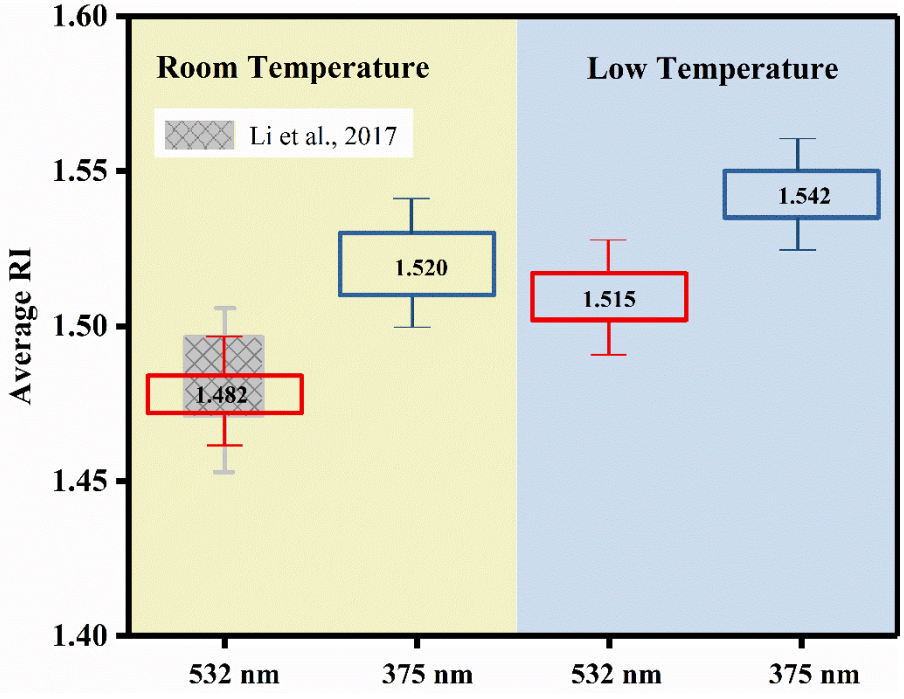

Figure 1. Summary of the averaged RI values of dodecane SOA under room temperature 25 ˚C (the light orange area) and low temperature 5 ˚C (the light blue area) in the wavelength of 532 nm and 375 nm. The red box is the averaged RI value for *n*-dodecane in 532 nm, the shaded boxes are the RI values from our previous study in 532 nm,(Li et al., 2017a) the blue box is the averaged RI value for *n*-dodecane in 375 nm.

https://doi.org/10.5194/acp-2019-1218
Preprint. Discussion started: 13 February 2020

Atmospheric Chemistry and Physics Discussions

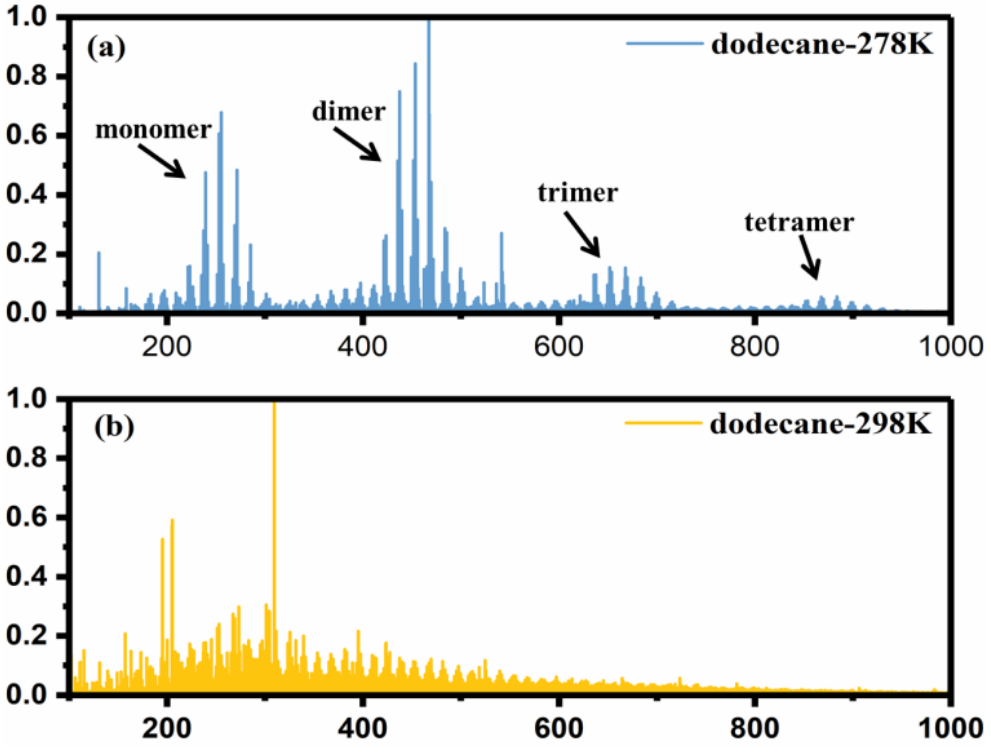

Figure 2. Mass spectra of *n*-dodecane SOA obtained by ESI-TOF-MS in positive ion mode. (a) low temperature condition; (b) room temperature condition.

https://doi.org/10.5194/acp-2019-1218
Preprint. Discussion started: 13 February 2020

Atmospheric Chemistry and Physics Discussions

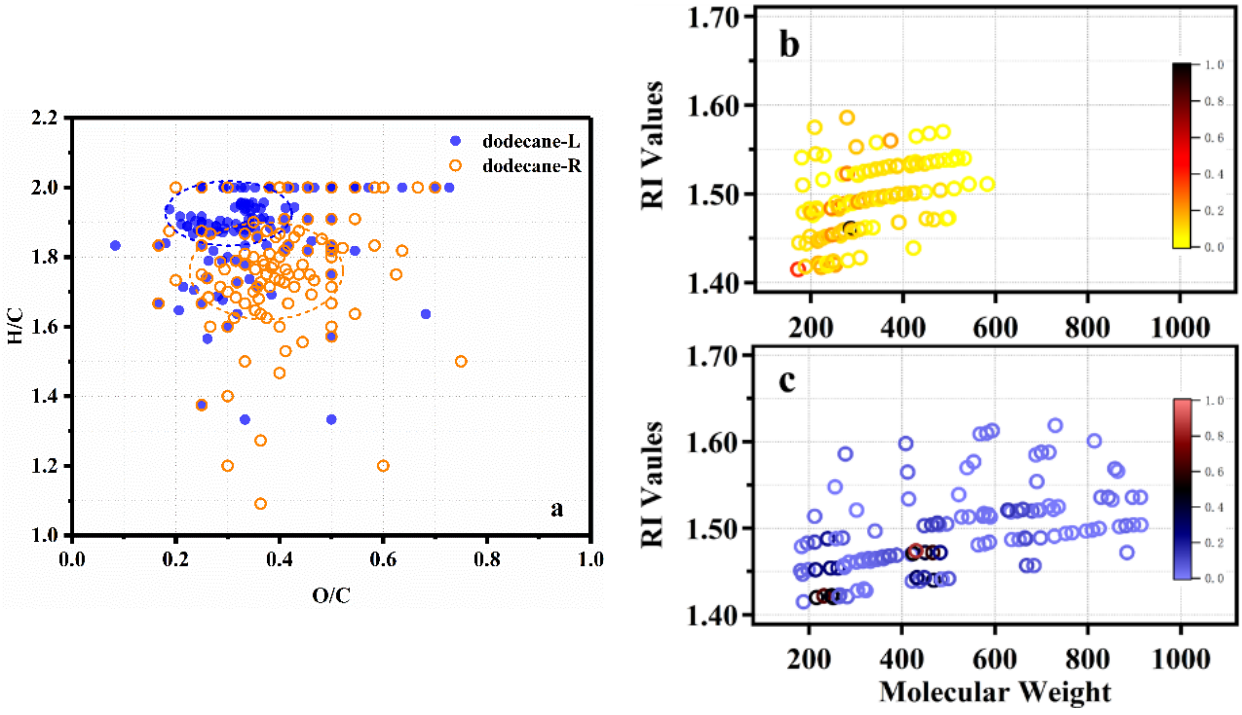

Figure 3. (a) Van Krevelen plots showing O/C and H/C ratios for identified products by EST-TOF-MS: the orange circle is for the SOA generated under room temperature condition; the blue circle is for the SOA generated under low temperature condition; (b) calculated RI values of the selected identified molecular species from MS spectra under room temperature, the color map refers to the relative intensity of the molecular formula; (c) calculated RI values of the selected identified molecular species from MS spectra under low temperature, the color map refers to the relative intensity of the molecular formula.

https://doi.org/10.5194/acp-2019-1218
Preprint. Discussion started: 13 February 2020

Atmospheric Chemistry and Physics Discussions

575

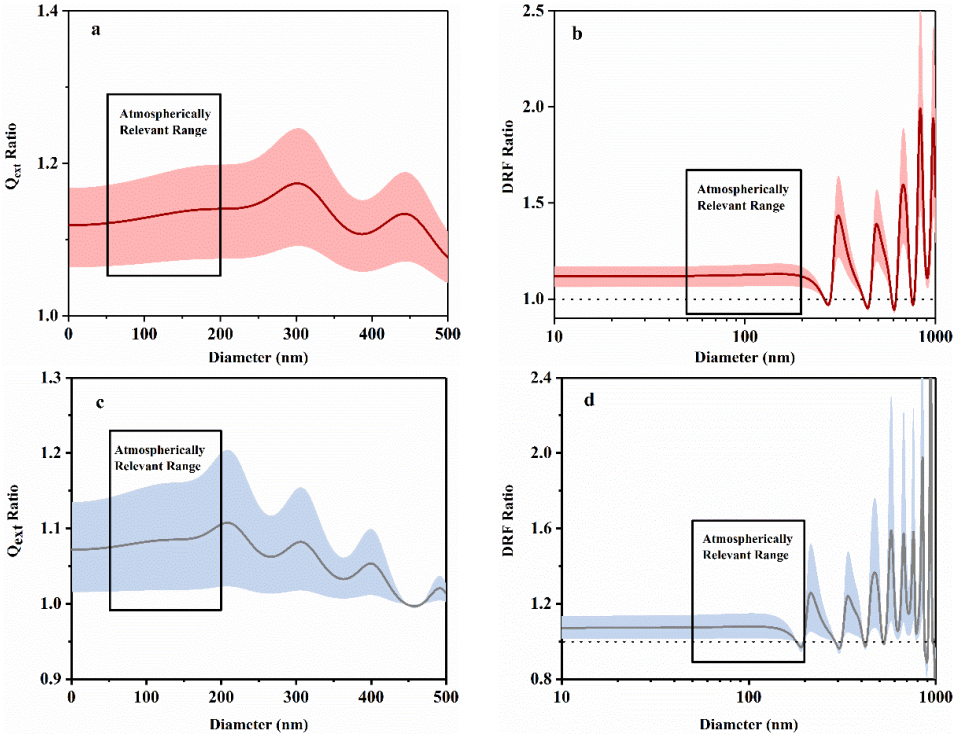

Figure 4. The ratio of light extinction efficiency (Q_{ext} ratio) and direct radiative forcing (DRF ratio) of *n*-dodecane SOA under different temperature conditions. (a) Q_{ext} ratio at 532 nm; (b) DRF ratio at 532 nm; (c) Q_{ext} ratio at 375 nm; (d) DRF ratio at 375 nm. The solid line is the average value of the ratio, and the shaded area is the uncertainty.

580